

See discussions, stats, and author profiles for this publication at: <https://www.researchgate.net/publication/343178579>

Flight Coordination of MAVs in GPS-denied Environments using a Metric Visual SLAM

Conference Paper · October 2019

CITATIONS

0

READS

46

2 authors:



Leticia Oyuki Rojas Pérez

Instituto Nacional de Astrofísica, Óptica y Electrónica (INAOE)

11 PUBLICATIONS 21 CITATIONS

[SEE PROFILE](#)



Jose Martinez-Carranza

Instituto Nacional de Astrofísica, Óptica y Electrónica (INAOE)

85 PUBLICATIONS 282 CITATIONS

[SEE PROFILE](#)

Some of the authors of this publication are also working on these related projects:



Modeling and Control of an Unmanned Aerial Manipulator (UAM) [View project](#)

Flight Coordination of MAVs in GPS-denied Environments using a Metric Visual SLAM

L. Oyuki Rojas-Perez ^{*1} and J. Martinez-Carranza^{1,2}

¹Instituto Nacional de Astrofísica, Óptica y Electrónica , Puebla, Mexico

²University of Bristol, Bristol, UK

ABSTRACT

Flight coordination of Micro Air Vehicles (MAVs) has become an essential task in the autonomous flight of swarms of drones. In recent years, we have seen demonstrations performed by giant companies such as Intel, where hundreds of drones perform a coordinated flight in the open sky. Although impressive, these demonstrations strongly depend on the use of GPS in order to effectively deploy MAVs in a co-ordinated fashion. In contrast, in this work, we present an approach for GPS-denied scenarios where localisation is resolved by using a well-known technique in robotics: visual simultaneous localisation and mapping. For this technique to be utilised, a single camera is mounted onboard the MAV, and even when a monocular camera is used to perform visual SLAM, if the camera angle w.r.t to the base of the drone and altitude are known, then the scale of the MAV's pose can be estimated. Rather than having a central controller, we have implemented a single individual controller for each drone involved in the coordinated flight. Thus, each drone knows its current drone's position as much as the position of its partner. This information is used in a PID controller with a consensus strategy to perform a coordinated flight defined by a set of waypoints. We showcase the effectiveness of our approach in an application where two drones have to carry an object from one location to another in a co-ordinated manner.

1 INTRODUCTION

Currently, MAVs are employed for the acquisition data from image areas with the purpose of generating 3-D models of an environment to evaluate infrastructures or contribute to cartographic information. There are some works that focus on complex tasks, where one MAV is insufficient to complete

^{*}Department of Computer Science at INAOE. Email addresses: {oyukirojas, carranza}@inaoep.mx



Figure 1: We present a methodology to perform an autonomous coordinate flight indoors using the same controller for both MAVs. We use the onboard monocular camera to metric localisation. A video of this work is found at <https://youtu.be/Tcox2MpRGrY>

an assignment such as exploration and inspection in vast territories, transportation of heavy loads or dangerous material. The latter calls for the use of more than one MAV, but also that such MAVs can cooperate during a mission flight.

The implementation of multiple MAVs requires the interaction between them to perform tasks in a coordinated manner. In this sense, MAV localisation is essential for cooperative tasks. For this reason, a research topic is that of estimating the drone's pose in 6D, which can be done by the use of GPS. However, GPS may not be accessible or reliable in some environments namely in urban canyons, forest environments or indoor scenes. [1], [2]. Motion capture systems are an alternative to GPS in terms of external localisation systems, however, this is not a general solution and therefore, there have been many efforts to develop systems to localise the drone via processing of sensor data acquired from onboard cameras, laser or similar sensors. The set of techniques relying on visual data for localisation are known as visual Odometry or visual Simultaneous Localisation and Mapping (SLAM), meaning that localisation is resolved while a map of the scene is also built.

Recently, visual SLAM has been used in the context of collaborative flight [3], where the authors present a cooperative system, a first drone navigates and maps the scene, while a second drone flies over the same place and recognises the

scene using the shared map by the first drone. In the other hand, the authors of [4] propose a method to fuse the IMU data and the monocular camera to build sub-maps for each MAV to get a robust communication between MAV's to perform efficient data exchange.

Motivated by the above, we present an autonomous system for multiple MAVs that uses a visual SLAM system to obtain the camera pose estimates with scale in centimetres for each MAV. The pose estimates are used by a PID controller with a consensus strategy to perform a coordinated flight defined by a set of waypoints.

The processing is carried out off-board since the MAV transmits the image and altimeter data in real time to a ground control station. Each MAV generates an individual metric map of the environment and shares its current position. For the flight, a predefined path in 3-dimensional coordinates is given, this path is followed by the coordinate MAV. We performed a series of experiments in indoor environments for the autonomous flight at 1.5 metres in height to transport a load in a straight line and for formation flight following a series of reference points, see the example in the Figure 1.

To present our proposed approach in detail, this paper has been organised as follows: section 2 describes the related work; section 3 describes our proposed methodology; 4 describes our experiments; finally, our conclusions are discussed in section 5.

2 RELATED WORK

The problem of collaborative or coordinated flight has been studied for several years now. One of the most common techniques is based on a leading-follower architecture. Some works have proposed the use of geometric relationships, speed ratio, minimum turning radius or potential fields as main strategy to implement the coordination [5]. Some works [6] present simulation experiments of the control of multiple unmanned aerial vehicles using the relative position of the leader, where two controllers modify the behaviour of the vehicles, the first one controls the trajectory that the vehicles must follow and the second controls the height of flight [7]. However, the vehicles maintain the formation under certain conditions, for example, constant speed and trajectory angle not greater than 20°[8].

Flight training has also been implemented based on global positioning and telemetry [9]. In its control station, information is monitored individually by the telemetry of each vehicle, which allows changing the parameters of the system to keep them aligned with their neighbours. Vehicles fly in two predefined courses at separate altitudes, where MAVs wait for others to join. When all the MAVs are in the arena, they fly to the predefined area [10]. Regarding the control algorithms, the leading vehicle receives commands of speed and angles of orientation and trajectory, while the follower follows the manoeuvres of the leader maintaining a distance of separation to avoid collisions, where the system of coordinates are

centred in the leading vehicle[11, 12]. In [13], the authors use a pilot to control the leading vehicle remotely, the control scheme consists of having to follow the leader under a separation distance. The primary condition of these works is that of maintaining the global position to remain in the formation.

On the other hand, the authors of [14], presage coordinated flight in interiors making complex trajectories. However, they depend on an external location system so that the vehicles stay aligned [15, 16, 1, 17, 18]. Besides, these works depend on the size of the arena to be able to carry out the training. In the works mentioned above the responsibility of the formation rests directly on the leading vehicle and this only receives information from the work station to update the trajectory, for the adjustment of parameters each follower vehicle receives updates individually.

In contrast to the works described before, in this work, an autonomous system is proposed to perform coordinated flight without dependency on the GPS. A strategy of consensus governs the proposed system. This enables the vehicles to make the flight without depending on a leader. Both vehicles receive the same parameters of speed and trajectory, as well as the same control system.

3 METHODOLOGY

The proposed autonomous system for multiple MAVs is based on two main components: (1)a metric monocular SLAM [19, 20] to obtain the camera pose estimates with scale in centimetres for each MAV;(2) and a Controller for Flight Coordination. Figure 2, shows the pipeline processing of our approach. The processing is carried out off-board since the MAV transmits the image and altitude data in real time to a Ground Control Station (GCS). Each MAV generates an individual metric map of the environment and shares its current position. For the flight, a predefined path in 3-dimensional coordinates is given, this path is followed by the MAVs.

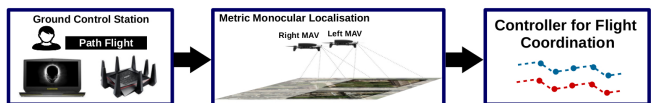


Figure 2: Schematic representation of our proposed approach. Two MAVs localise themselves by using our metric monocular system, where the camera looks down at the ground, while the camera images are processed to obtain the MAV's pose estimates.

3.1 Visual Metric Localisation

The Metric monocular SLAM is a modified version of RGB-D of ORB-SLAM. This method generates a synthetic depth image based on the line-plane intersection problem by formulating a geometric configuration where it is assumed that the ground is plane. The Bebop's altimeter is used to obtain an estimate of the camera's height h in centimetres and

the camera angle is obtained through the SDK is used to calculate the angle at which a vector n would be located with respect to the origin in the camera's coordinate system with length h . This vector n is perpendicular to the planar ground; therefore, it can be used to know a point lying on this planar ground with normal n . Figure 3 illustrates a side view of this geometric configuration when the bebop's camera is foveated to the angle of -30° with respect to the horizon. The line-plane intersection equations are used to find α , depth corresponding to the pixel x, y .

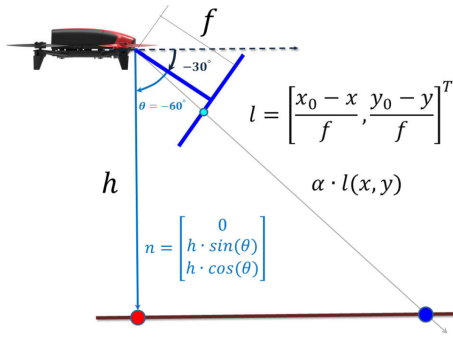


Figure 3: Geometric configuration used to generate a synthetic depth image to be used by ORB-SLAM in its RGB-D version, to obtain a pose estimation with metric. Image taken from [19].

3.2 Controller for Flight Coordination

The proposed controller uses rotation matrices to calculate the orientation of the current point with respect to the reference point, for which control commands are sent in yaw. The translation is calculated using the vector generated between the current point towards the reference point and to reach the desired point, and control commands are sent in pitch. To achieve a coordinated flight, the controller receives the position of the vehicle on the left and the one on the right, later a consensus strategy is implemented, which allows them to moderate their speed to keep them aligned during the flight. Once the vehicles arrive at the reference point, they are oriented towards the next one and later they are moved to the designated point. This will be calculated depending on the number of points of reference. The Robotic Operating System (ROS) communication system allows both vehicles to use the same control, under the same conditions, speed and path flight.

4 EXPERIMENTS

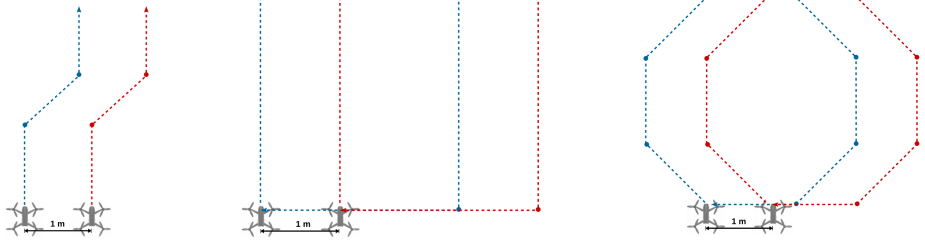
We present three different sets of experiments where we evaluated the performance of our proposed methodology. In these experiments, the vehicles take off and perform autonomous flight in an indoor environment by following a trajectory defined by a user. We evaluated the accuracy of the coordinate flight, for these, we used the motion capture system Vicon to obtain the measurements of the MAV's position.

For our experiments, we used two Parrot Bebop 2.0 Power Edition. We used the images captured with the onboard camera transmitted via WiFi with a resolution of 640 x 368 pixels at 30 Hz and the altimeter data transmitted at 5 Hz. Communication is possible using a router to communicate both vehicles to the GCS. For the programming of the controller, we used the Software Development Kit (SDK) known as the bebop autonomy SDK. This package run on a GCS: an Alienware-Dell Laptop with Intel Core-i7, with 16 GB in RAM. We used the ROS, Kinetic version, for implementation of our approach and communication with the other nodes; the Bebop driver, metric monocular SLAM and our controller. Figure 5, shows a scheme of our software architecture. Our approach uses the same flight controller for both MAVs. For the latter we exploited the capabilities of node reconfiguration offered by ROS through the use of the launcher files. In addition, ROS also facilitated the communication, transmission and consumption of all the data involved in our system, which led to carry out coordinated successful flights.

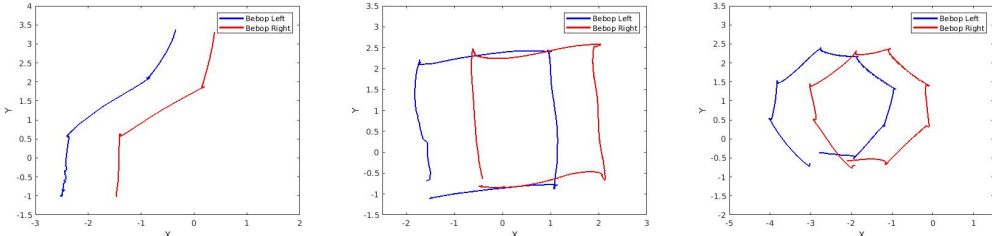
Figure 4(a), shows three plan flights: Line, Square and Octagon. The first trajectory is composed of three waypoints, the second trajectory is composed of four waypoints and the third trajectory has eight waypoints. The vehicles start 1 metre apart. After takeoff, each vehicle confirms if its partner is ready to start the flight. First, each vehicle changes heading in the direction of the next waypoint, once oriented, the PID controller calculates the error w.r.t. the next waypoint and sends control commands to pitch in order to fly towards this waypoint. For the consensus strategy, the controller receives information about the position of its partner and calculates the difference in the X coordinate (front axis). This difference value is added up to the pitch controller in order to regulate the speed of each drone in order to wait for each other or speed up, aiming at maintaining the same distance towards the waypoint. When the waypoint is reached, the controller turns the vehicle in the direction of the next waypoint. This will continue until each MAV reaches the last waypoint and then each one will land. Figure 4(b), shows the trajectories performed by the MAVs, the trajectories demonstrate that the vehicles follow the path symmetrically.

Ten runs of each trajectory were made. Table 1 shows that, on average, vehicles maintain the initial separation distance. The evaluation made of the trajectories with the VICON motion capture system was divided into two tables, table 2 corresponds to the vehicle on the left and table 3 corresponds to the vehicle on the right. In them, it can be seen that the error of the line path is high, due to the disturbances that are generated between them. However, in the square and octagon trajectories, it can be seen that the average error is less than 2%.

Figure 6, shows the trajectories generated with the coordinated flight controller, first shows the results of the vehicle on the left, followed by the results of the vehicle on the right. The first two columns show 5 line trajectories, column three



(a) Tracks designed to evaluate the autonomous coordinate flight.



(b) Trajectories performed by the MAVs evaluated using VICON.

Figure 4: Tracks predefined to perform coordinate flight, the blue line represent the left MAV trajectory and the red line correspond to the right MAV.

and four show 5 square trajectories and the last two columns show five octagon trajectories. The red line indicates the trajectory followed by the vehicle and the green line indicates the ground truth (VICON). Although there are disturbances generated between them, the vehicles are able to carry out the desired trajectory successfully.

Finally, the Figure 7 external views of the autonomous flight execution are displayed using the coordinated flight controller. The first row shows the performance of the line trajectory. The second row corresponds to the square trajectory; the third row shows the performance of the octagon trajectory. Finally, an example of cooperative flight is shown using the coordinated flight controller proposed in this work, Figure 8.

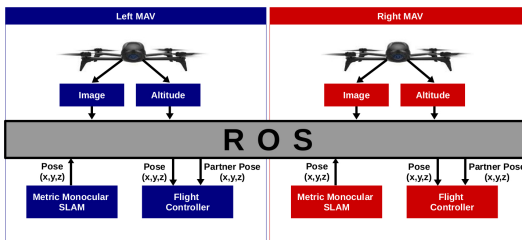


Figure 5: The architecture of the processing of our approach using ROS as a communication channel. Each PID controllers know the metric position of the partner to compensate the differences of the current pose to the reference point, this allows the flight are coordinate.

Table 1: Average Distance Between MAVs During Coordinated Flight.

Trajectory	Average distance [m]	Std [m]
Line	1.032	±0.110
Square	1.084	±0.197
Octagon	1.002	±0.171

Table 2: Left MAV

Trajectory	Average Error [m]	Std [m]	Average traversed distance [m]	Error in %
Line	0.120	±0.067	5.825	2.532
Square	0.159	±0.089	13.111	1.213
Octagon	0.218	±0.110	11.636	1.871

5 CONCLUSION

We have presented the implementation of a single individual controller for each MAV involved in a coordinated flight. So each MAV knows its current position as well as the position of its partner. This information is used in a PID controller with a consensus strategy, which commands each drone to follow a flight plan made of a set of waypoints. The results of the evaluation show that the average error of the estimated trajectories followed by each MAV is, in average, below 2% of the total trajectory, this in comparison to ground truth obtained with a motion capture system. In addition, we have presented an illustrative application where two MAVs are co-

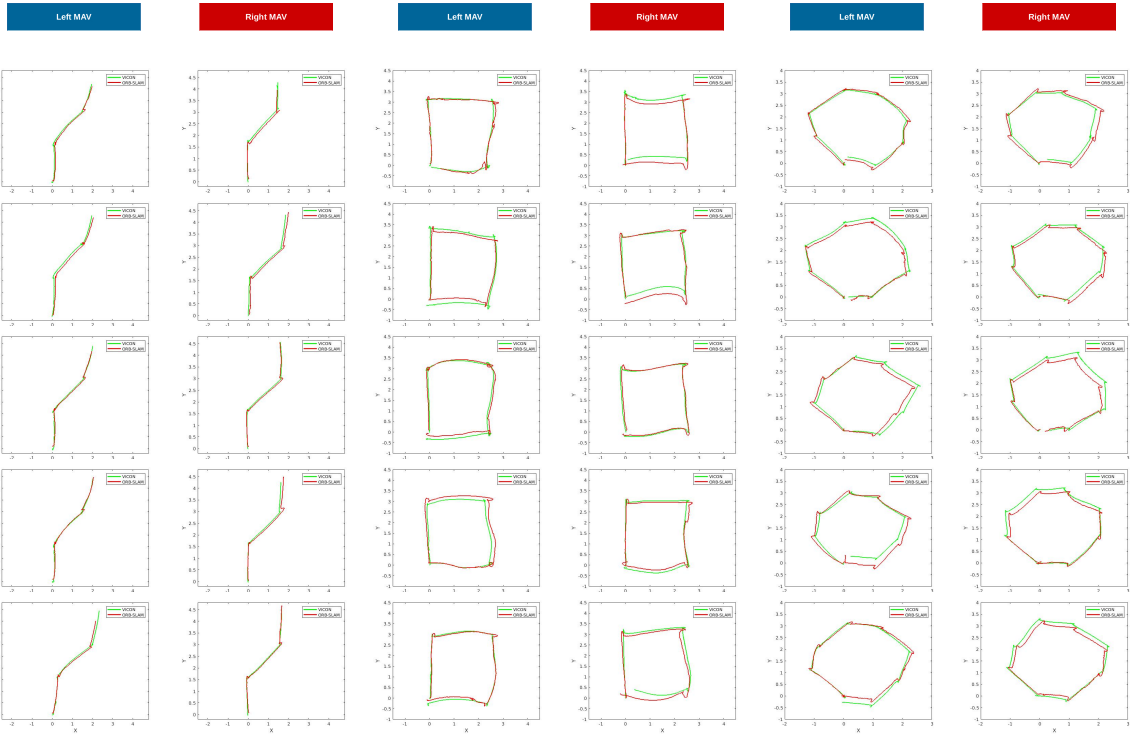


Figure 6: Examples of the trajectories generated. The green line represents the ground truth (VICON), and the red line is the path travelled by the vehicle. First, the graph of the vehicle placed on the left is shown, depending on the vehicle placed on the right.

Table 3: Right MAV

Trajectory	Average Error [m]	Std [m]	Average traversed distance [m]	Error in %
Line	0.155	±0.080	5.662	2.732
Square	0.179	±0.107	12.008	1.493
Octagon	0.162	±0.078	11.156	1.456

ordinated, using our approach, to carry out a collaborative flight to transport a load without risk of collision. We believe that the obtained results are promising and we will continue working on expanding the control for more than two MAVs, improving the communication system between them and the control algorithm.

REFERENCES

- [1] A. Kushleyev, D. Mellinger, C. Powers, and V. Kumar. Towards a swarm of agile micro quadrotors. *Autonomous Robots*, pages 287–300, 2013.
- [2] G. Vásá, Cs. Virág, G. Somorjai, N. Tarcai, T. Szörényi, T. Nepusz, and T. Vicsek. Outdoor flocking and formation flight with autonomous aerial robots. In *IEEE/RSJ IROS*, pages 3866–3873. IEEE, 2014.
- [3] P. Schmuck. Multi-uav collaborative monocular slam. In *Robotics and Automation ICRA*, pages 3863–3870. IEEE, 2017.
- [4] N. Mahdoui, E. Natalizio, and V. Fremont. Multi-uavs network communication study for distributed visual simultaneous localization and mapping. In *ICNC*, pages 1–5. IEEE, 2016.
- [5] T. Paul, T. Krogstad, and Jan T. Gravdahl. Modelling of uav formation flight using 3d potential field. *Simulation Modelling Practice and Theory*, pages 1453–1462, 2008.
- [6] F. Giulietti, L. Pollini, and M. Innocenti. Autonomous formation flight. *IEEE-Control Systems Magazine*, pages 34–44, 2000.
- [7] Q. Zhang and H. H. T. Liu. Robust nonlinear control of close formation flight, 2019.
- [8] M. Pachter, J. D’Azzo, and Andrew W. Proud. Tight formation flight control. *Journal of Guidance, Control, and Dynamics*, pages 246–254, 2001.
- [9] G. Vásárhelyi, C. Virág, G. Somorjai, N. Tarcai, T. Szörényi, T. Nepusz, and T. Vicsek. Outdoor flocking and formation flight with autonomous aerial robots. In *2014 IEEE/RSJ IROS*, pages 3866–3873, 2014.



Figure 7: Examples of autonomous flight performed in a real-time on the indoor environment. The first row corresponds a line trajectory, the second row, correspond a square path and the third row, correspond an octagon trajectory.



Figure 8: Examples of autonomous collaborative flight performed in a real-time on the indoor environment.

- [10] W. Meng, Z. He, R. Su, P. K. Yadav, R. Teo, and L. Xie. Decentralized multi-uav flight autonomy for moving convoys search and track. *IEEE Transactions on Control Systems Technology*, pages 1480–1487, 2017.
- [11] D. Casbeer, S. Rasmussen, D. Kingston, D. Baker, and E. Garcia. Implementation of leader-wingman flight formation with sampled-data controller. In *AIAA Scitech Forum*, page 1453, 2019.
- [12] C. Schumacher and S. Singh. Nonlinear control of multiple uavs in close-coupled formation flight. 2000.
- [13] Y. Gu, B. Seanor, G. Campa, M. R. Napolitano, L. Rowe, S. Gururajan, and S. Wan. Design and flight testing evaluation of formation control laws. *IEEE Transactions on Control Systems Technology*, pages 1105–1112, 2006.
- [14] M. Turpin, N. Michael, and V. Kumar. Trajectory design and control for aggressive formation flight with quadrotors. *Autonomous Robots*, pages 143–156, 2012.
- [15] J. Welsby, C. Melhuish, and C. Lane. Autonomous minimalist following in three dimensions: a study with small-scale dirigibles. *Proceedings of Towards Intelligent Mobile Robots Manchester*, 2001.
- [16] G. Hoffmann, H. Huang, S. Waslander, and C. Tomlin. Precision flight control for a multi-vehicle quadrotor helicopter testbed. *Control Engineering Practice*, pages 1023 – 1036, 2011. Workshop on Dependable Control of Discrete Systems.
- [17] M. Turpin, N. Michael, and V. Kumar. Decentralized formation control with variable shapes for aerial robots. In *2012 IEEE Robotics and Automation*, pages 23–30, May 2012.
- [18] T. Stirling, J. Roberts, Jean-C. Zufferey, and D. Floreano. Indoor navigation with a swarm of flying robots. *Robotics and Automation*, pages 4641–4647, 2012.
- [19] H. Moon. Challenges and implemented technologies used in autonomous drone racing. *Intelligent Service Robotics*, 12(2):137–148, Apr 2019.
- [20] L. O. Rojas-Perez and J. Martinez-Carranza. Metric monocular slam and colour segmentation for multiple obstacle avoidance in autonomous flight. In *RED-UAS*, pages 234–239, Oct 2017.